

Shear Behaviour of Rock Joints Under CNL and CNS Boundary Conditions

Amit Kumar Shrivastava  · K. Seshagiri Rao

Received: 22 October 2014 / Accepted: 16 May 2015 / Published online: 23 May 2015
© Springer International Publishing Switzerland 2015

Abstract Shear behaviour of rock joints can be studied under both constant normal load (CNL) and constant normal stiffness (CNS) boundary condition. CNS condition is suitable for non planar and reinforced rock joints whereas CNL condition is suitable for planar and non reinforced rock joints. In the present study shear behaviour of modelled rock joints with different asperity have been experimentally investigated under both CNL and CNS boundary conditions. Test results indicate that CNS boundary conditions gives higher shear strength as compare to CNL boundary condition when other parameter of testing is kept same. But, this effect tends to diminishes with increase in normal stress on the shearing plane and at high normal stress both CNL and CNS boundary conditions gives same shear strength. A new shear strength model is proposed for both the boundary condition and the proposed model is validated by comparing the predicted shear strength with present experimental results and results available in the literature for natural and artificial rock joints with different asperity and roughness. The new study and

model will be useful for safe and economical design of underground openings in jointed rocks, stability analysis of rock slopes, design of foundation on rock and design of rock socketed piles.

Keywords Shear strength · Dilation · Constant normal load · Constant normal stiffness · Modelling · Physical modelling

1 Introduction

Rock is heterogeneous and discontinuities are inevitable part of the rock masses. The presence of these discontinuities in the rock mass is in the form of joints, faults, bedding planes or other recurrent planar fractures. The presence of these discontinuities reduces the shear strength and influences shear behaviour. In addition to joints, shear behavior of the rock mass also influenced by various parameters like, joint roughness, stiffness of the surrounding rock mass, shear rate, condition of the joint i.e. unfilled/infilled, infill type and their thickness. The correct evaluation of shear behavior of rock mass is only possible if all these factors are considered during experimental, analytical and numerical studies. The correct evaluation of shear behavior of rock joints is important for safe and economical design of underground openings in jointed rocks, stability analysis of anchored/free rock slopes, risk

A. K. Shrivastava (✉)
Department of Civil Engineering, Delhi Technological
University, Bawana Road, New Delhi 110042, India
e-mail: aksrivastava@dce.ac.in

K. S. Rao
Department of Civil Engineering, Indian Institute of
Technology, Delhi, Hauz Khas, New Delhi 110016, India
e-mail: raoks@civil.iitd.ac.in

assessment of underground waste disposal, design of foundation on rock and design of rock socketed piles (Rao et al. 2009).

The shear behavior can be investigated broadly under two different boundary conditions i.e. constant normal load (CNL) and constant normal stiffness (CNS). The shearing under CNL boundary conditions are suitable for situations: (1) planar joints, where no dilation takes place during the shearing process, (2) non planar and unreinforced rock slope where the surrounding rocks freely allow the joints to shear without restricting the dilation, thereby keeping normal load constant during shearing process. If the dilation of rock joints is either partly or fully restricted by the surrounding rock mass or reinforcement provided at the joints during the shearing process than there will be change in the normal load on the shearing plane. This change in the normal load on the shearing plane depends upon the stiffness of the surrounding rock mass or reinforcement provided and dilation resisted, hence shearing will take place under variable normal load condition, which can be simulated as CNS boundary conditions. Stiffness is the material property, which is constant for a given rock mass at a particular depth. As mostly rock joints are non planar and reinforcements are provided to the rock joints to increase the stability, hence a more representative behavior of joints would be achieved if shear behavior is investigated under CNS boundary conditions.

Conventional equipment used by different scholars (Newland and Allely 1957; Patton 1966; Goldestin et al. 1966; Ladanyi and Archambault 1970; Barton 1973; Byerlee 1975; Yang and Chiang 2000; Saiang et al. 2005; Ghazvinian et al. 2010) in previous days fails to explain correctly the shear behavior of rough and reinforced rock joints because of the limitation of boundary conditions, these equipment work under CNL boundary condition only. The shear strength model proposed by them based on these studies fails to predict shear strength correctly because of the limitation of boundary conditions.

To overcome this limitation, either conventional equipments were modified by Obert et al. (1976) and Ooi and Carter (1987) or new equipment developed by Indraratna et al. (1998) or servo controlled equipment developed by Jiang et al. (2004) and Kim et al. (2006) to conduct tests under CNS boundary conditions. The equipment modified or developed by Obert et al. (1976), Ooi and Carter (1987) and Indraratna et al.

(1998) have difficulties to change the reaction rods, beams and stiffness plate to simulate different stiffness conditions according to the stiffness of the surrounding rock mass, while changing there is also a chance that sample may fail before testing of samples start. These difficulties have been overcome by using servo controlled equipment such as used by Jiang et al. (2004), but this equipment is suitable for comparatively smaller size of sample, due to that influence of joint roughness cannot be well studied and there is no facility to measure the rotation of the sample. The equipment developed by Kim et al. (2006) can test the samples only under two extreme conditions of stiffness of the boundary i.e. CNL (normal stiffness $k_n = 0$) and infinite normal stiffness condition ($k_n = \infty$). Servo control large scale direct shear testing machine designed by Shrivastava and Rao (2013) is capable of conducting tests on large and jointed prismatic specimens through friction free rigid platens under CNL and CNS boundary conditions, which can test under any condition of stiffness of the boundary without using or changing the reaction rods, beams and stiffness plates.

The present study will explain the effect of the joint roughness and boundary conditions on the shear behavior of the rock joints and suitable failure criteria will be proposed.

2 Testing Equipment

A servo control large scale direct shear apparatus designed and developed by Shrivastava and Rao (2013) is used for testing the rock joint under CNL and CNS boundary conditions. The apparatus consists of three main units such as loading unit, hydraulic power pack with servo valve and data acquisition and controlling unit as shown in Fig. 1. The loading unit consist of two shear box of size 300 mm × 300 mm × 448 mm having a gap of 5 mm between the boxes. The needle linear bearing of 5 mm thickness is placed between the shear boxes to maintain the 5 mm gap between the boxes and avoid any frictional forces during shearing to the sample. The upper shear box is fixed and the joint is sheared by moving the lower box. The upper box can only move in the vertical direction. The lower box is fixed on a rigid base through bearings, which can move only in horizontal direction. The apparatus is fitted with two actuators for load and six LVDTs for displacement



Fig. 1 Photograph of large scale direct shear testing machine

measurements. The normal and shear load is applied uniformly on the shearing plane through the load cell of the capacity of 500 and 1000 kN respectively. Displacements are monitored and measured through six number of LVDTs. Four LVDTs are used to measure the normal displacement and to provide a check on specimen rotation about an axis parallel to the shear zone and perpendicular to the shearing direction. Degree of joint closure and dilation angle can also be obtained from these measurements. Two LVDTs are used to measure the shear displacement. These displacement devices have adequate ranges of travel to accommodate the displacements, ± 20 mm. Sensitivities of these devices are 0.001 mm for both normal displacement and shear displacement.

The second unit of apparatus consists of hydraulic power pack with servo valve, the function of the hydraulic power pack is to supply required flow and pressure for the actuation of the actuator and the function of servo valve is to control the flow of the hydraulic fluid to the actuator.

Data acquisition and controlling unit is the third unit of apparatus. Data acquisition system consists of a computer installed with direct shear test software and PCI bus advanced data acquisition card. The output of data acquisition system is connected to CPU via cord and the load and deformation values are stored at desired intervals as notepad data. The software is having the capability to control the test, collect the data and plot online graph between shear load versus time, normal load versus time, shear load versus

normal load, shear load versus shear displacement, normal load versus normal displacement and shear displacement versus normal displacement. Controlling unit consists of signal conditioning unit and controlling unit. Signal conditioning unit receives the output signal from the various transducers which amplifies and process the signal as per the requirement and transfer it to computer through connecting cables where it is accepted by the data acquisition system. The detailed working of this equipment is presented in Shrivastava and Rao (2013).

In this apparatus, CNL and CNS conditions are achieved by an electro hydraulic servo-valve, which controls the application of hydraulic power to linear actuator to provide the programmed normal force to test specimens. The programmed normal force is calculated from the Eq. (1), as proposed by Shrivastava and Rao (2013). The Eq. (1) is also made the part of direct shear testing software which is used for monitoring, recording and plotting the test results. The asperity angle (i), initial normal load (P_n) and stiffness of the rock joints or reinforcement (k_n) is feeded as input data in the direct shear testing software. The dilation and horizontal displacement data collected through sixteen channel data acquisition system is also feeded to direct shear testing software. The increased load during the progress of testing is calculated by the following equation:

$$P_{n(t+\Delta t)} = P_{n(E)} + k_n(Y - Y') \tag{1}$$

where $P_{n(t+\Delta t)}$ = normal force at any time interval $t + \Delta t$, $P_{n(t)}$ = normal force at any time interval t , k_n = stiffness of the surrounding rock mass, $Y - Y'$ = dilation resisted by the surrounding rock mass, Y = free dilation at any shear deformation.

The typical calculation for a given asperity angle (i) is as shown in Fig. 2, $Y = X \tan i$ when sample is

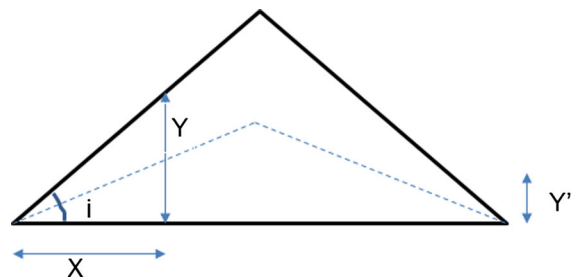


Fig. 2 Typical asperity profile

free to dilate, from the given JRC value the equivalent i value can be calculated by the method suggested by Xie and Pariseau (1992) and Maksimovic (1996), X = horizontal displacement measured as the average of two horizontal LVDT's placed near the sample, Y' = dilation measured as the average of readings of four normal LVDT's placed on the top of the sample.

3 Physical Modeling

3.1 Selection of Model Material

It is difficult to interpret the result of direct shear test on natural rock because of difficulties in repeatability of the sample. To overcome this problem a model material is selected which can be easily handled and reproducibility of the sample can be ensured. Plaster of Paris (POP) is selected because of its universal availability and its modulability into any shape when mixed with water to produce the desired joints and also long term strength is independent of time once the chemical hydration is completed.

To perform a series of physical and mechanical tests a number of specimens were prepared by mixing the prescribed quantity of water with POP powder. The prescribed percentage of water is decided so as to achieve proper workability of the paste and required strength to simulate soft rock. The different water powder ratio is tried and the desired strength and workability is obtained with water powder ratio of 0.60. The resultant paste after 1–2 min of mixing was poured into aluminum cylindrical moulds. The sample is removed from the mould after about 30–40 min of pouring, so that sample gets sufficiently hardened and

stand freely for curing in air. Now, the specimens were air cured at room temperature for 14 days before testing. Initial size of the specimen was 38 mm in diameter and 76 mm in height, which is used for unconfined compressive strength tests. The samples for other tests are cut from this samples depending upon size requirements.

The basic properties of the model material like dry density (Υ_d), uniaxial compressive strength (σ_c), Poisson's ratio (ν) and tangent modulus (E_{t50}) were determined in the laboratory as per the suggested methods ISRM (1977, 1979). The basic properties of the model material at 60 % of the moisture are presented in Table 1. The average uniaxial compressive strength of model material is 11.75 MPa and average tangent modulus at 50 % of peak axial stress is estimated 2281 MPa. Thus, the material can be classified as 'EL' based on Deere and Miller (1966) classification chart, indicating that the material is of very low strength (E) and low modulus ratio (L) and is suitable for simulating the behaviour of jointed rocks like siltstone, sandstone, friable limestone, clay shale and mudstone.

3.2 Sample Preparation

The sample with different asperity and roughness is prepared with the help of specially designed and fabricated casting mould and asperity plate, both is of cast iron. The rock joint is seldom plane, it always contains roughness and joint roughness can be of any shape and size. The roughness can vary within the joints or it will be different for different joints. The physical modelling of joint roughness as it appears in the in situ rock joints is very difficult. Hence, in the

Table 1 Properties of model material

Property	Sample description	No. of samples	Representative value	Testing method
Dry density, Υ_d (kN/m ³)	38 mm diameter, 76 mm height cylinder	20	12.34	ISRM (1977)
Uniaxial compressive strength (intact cylinder), σ_c (MPa)	38 mm diameter, 76 mm height cylinder	12	11.75	ISRM (1979)
Poisson's ratio, ν	38 diameter, 76 mm height cylinder	3	0.22	ISRM (1979)
Tangent modulus, E_{t50} (MPa)	38 mm diameter, 76 mm height cylinder	3	2281	ISRM (1979)
Modulus ratio (E_{t50}/σ_{ci})	–	3	194	ISRM (1979)
Failure strain in UCS, ϵ_f (%)	38 mm diameter, 76 mm height cylinder	3	0.63	ISRM (1979)
Deere–Miller (1966) classification	–	–	EL	

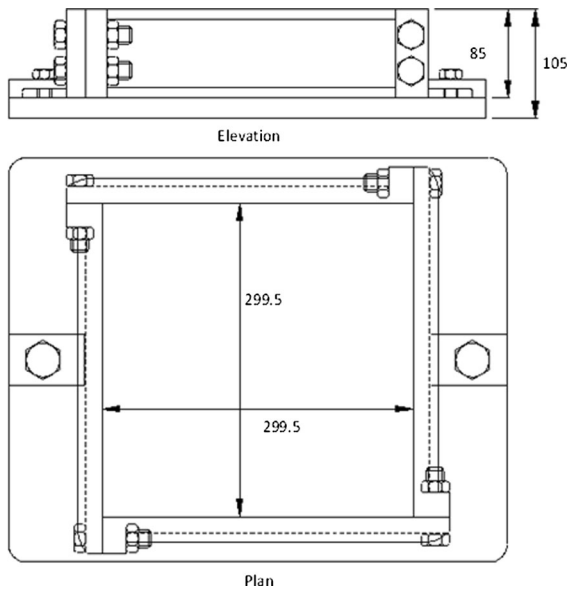


Fig. 3 Schematic diagram of casting mould

present work joint of equal and unequal angle asperity is prepared with the help of specially designed casting mould size $299.5 \times 299.5 \times 85$ mm (Fig. 3) and asperity plate of angles $0^\circ-0^\circ$, $30^\circ-30^\circ$, $15^\circ-15^\circ$ and $30^\circ-15^\circ$. The schematic diagram and photograph of one of the asperity plate of angle $15^\circ-15^\circ$ is shown in Fig. 4. These asperity angles can easily be converted into joint roughness coefficient (JRC) value by the use

of method suggested by Xie and Pariseau (1992) and Maksimovic (1996).

The two parts namely upper and lower, parts of the joints are prepared simultaneously to create proper mated joints. The casting moulds with suitable platform is placed and screwed properly on the vibrating table. The desired asperity plate is placed inside the mould facing the inclined asperity surface upwards. POP mixed with water thoroughly for 2 min before pouring into the casting mould, by maintaining the water POP ratio as 0.60 and the paste is then vibrated on vibrating table for 1 min to compact and to remove any entrapped air. The top surface of the specimen is properly leveled and excess paste is removed. The samples require 55 min to achieve final setting; hence, sample is removed from the mould only after elapse of 55 min after adding water into the POP, so as to insure proper shape of the sample. The samples are allowed to cure in air for 14 days before testing. The different roughness conditions of the rock joints were simulated by preparing four types of specimen sets namely $0^\circ-0^\circ$, $30^\circ-30^\circ$, $15^\circ-15^\circ$ and $30^\circ-15^\circ$, the sample with asperity $30^\circ-30^\circ$, $15^\circ-15^\circ$ and $30^\circ-15^\circ$ are presented in Fig. 5.

3.3 Experimental Investigation

The shear behaviour of joints under CNL condition was investigated before joints were tested under CNS

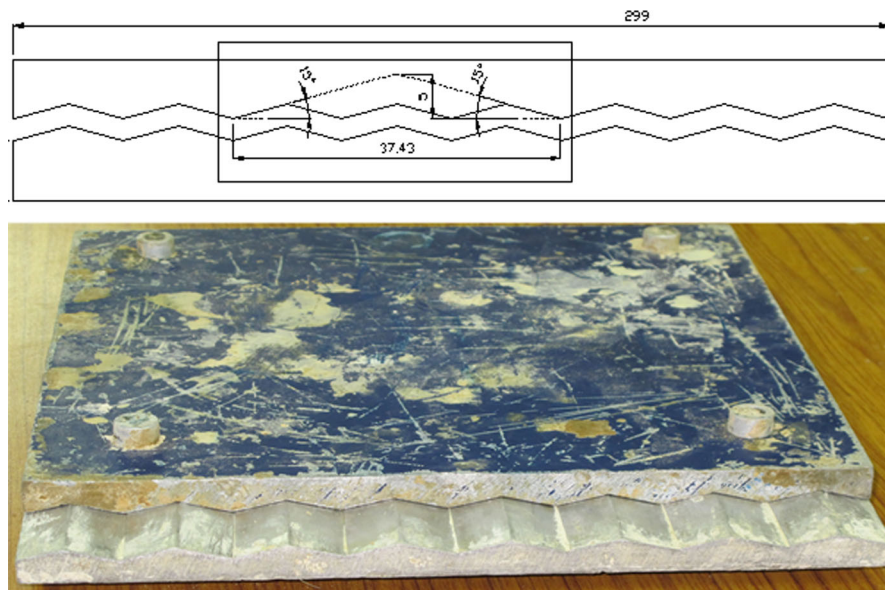


Fig. 4 Schematic diagram and photograph of asperity $15^\circ-15^\circ$ (all dimensions are in mm)

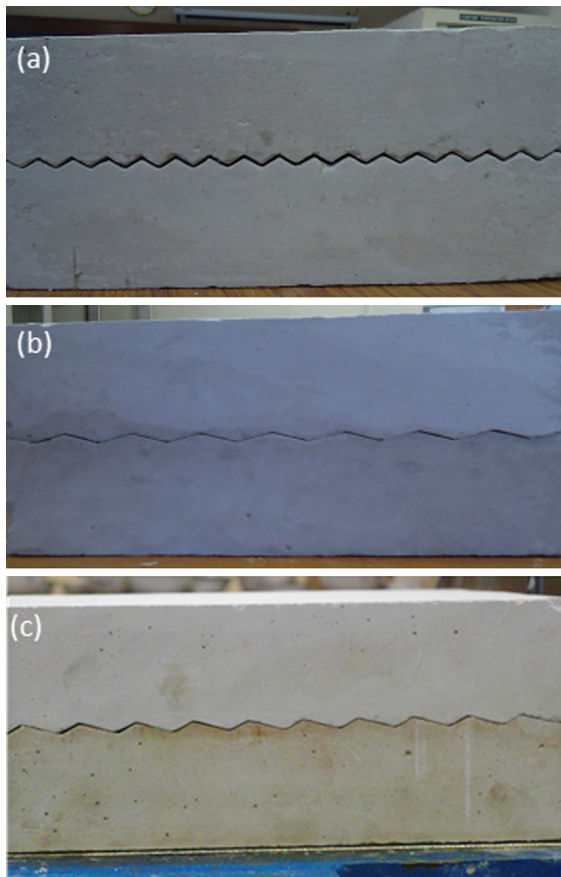


Fig. 5 Photograph of samples with asperity 30° – 30° , 15° – 15° and 30° – 15°

conditions. This has been carried out to assess the affect of boundary conditions on the shear behaviour. Hence, a series of tests were performed on the physically modeled rock joints with asperity angles 30° – 30° , 15° – 15° and 30° – 15° . To study the affect of the asperity on shear behaviour, tests were also performed on planar joints with asperity angle 0° – 0° for the boundary conditions, complete test, summary of the tests programme is presented as flow chart in Fig. 6.

In the present study 0.50 mm/min rate of shearing is selected, which is based on the study carried out by Shrivastava (2012) on similar type of physically modeled rock joints, where it has been concluded that there is no effect of shearing rate on peak shear stress up to shearing rate of 0.5 mm/min and at shearing rate more than 0.5 mm/min the effect is to increase the peak shear stress for both the boundary conditions.

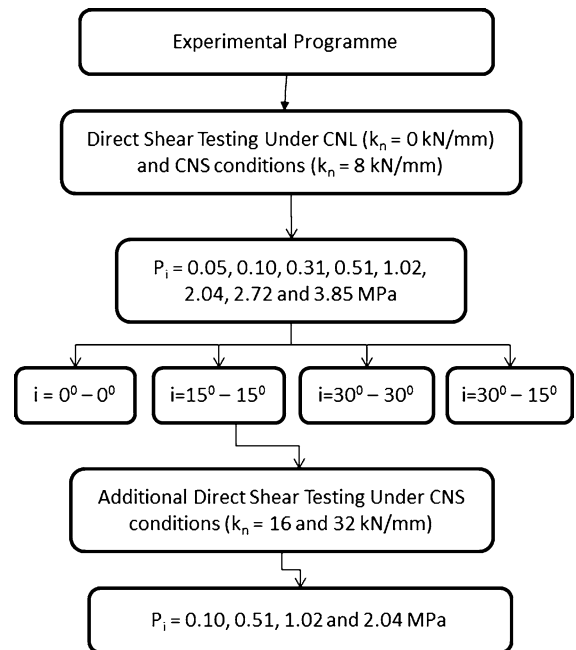


Fig. 6 Experimental programme

The effect of CNS boundary conditions on shear behaviour is discussed in detail by Shrivastava and Rao (2010, 2011) and Shrivastava et al. (2011).

3.3.1 Shear Behaviour

The shear behaviour of 30° – 30° , 15° – 15° and 30° – 15° asperity joint under CNL ($k_n = 0$ kN/mm) and CNS ($k_n = 8$ kN/mm) boundary condition is plotted as shown in Figs. 7, 8 and 9. To get the normal and shear stress normal load and shear load is divided by the initial cross sectional area of the sample. The stress–displacement behaviour is characterized by a well defined peak. It is clear from the test result that CNL boundary condition always under predicts the shear strength of the joint as compared to CNS boundary condition for the same initial normal stress. The shear stress response for planar joints under various P_i is presented in Fig. 10. The stress–displacement behaviour is characterized by increase in the shear stress with shear displacement till peak is reached and thereafter shear stress is found to be constant. The peak is reached when the shear stress almost equal to the normal stress acting on the joint. The constant shear stress indicates sliding of the sample on the failure surface. The CNS condition is not possible for

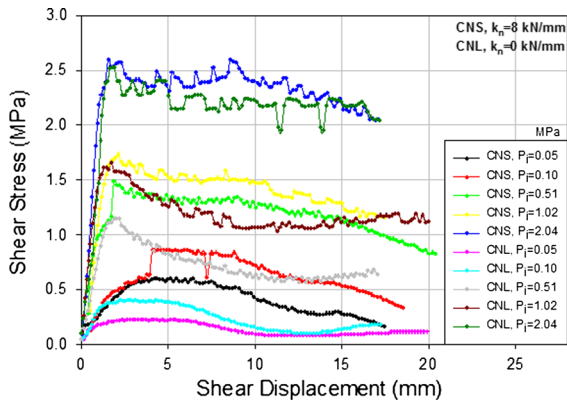


Fig. 7 Shear behaviour of 30°–30° asperity joint under CNL and CNS boundary condition

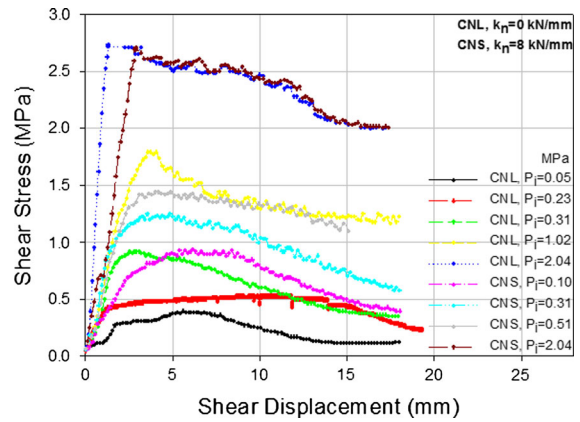


Fig. 9 Shear behaviour of 30°–15° asperity joint under CNL and CNS boundary condition

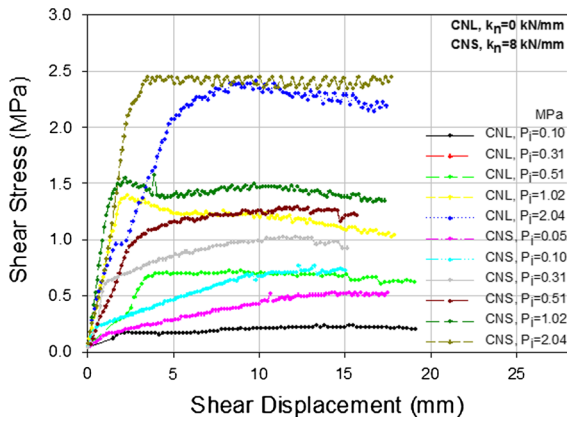


Fig. 8 Shear behaviour of 15°–15° asperity joint under CNL and CNS boundary condition

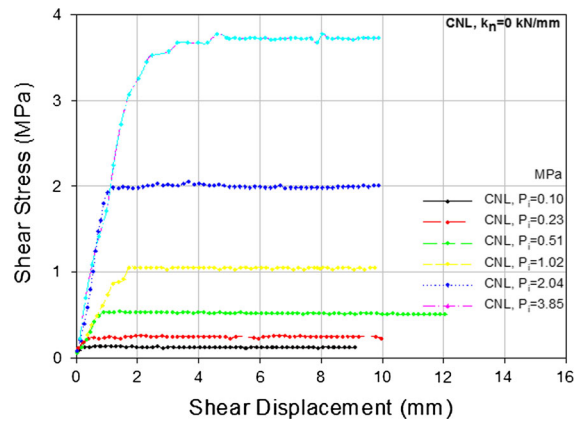


Fig. 10 Shear behaviour of planar joint

planar joint because for planar joint $Y = 0$ and $P_{n(t)}$ will be equal to $P_{n(t+\Delta t)}$, which can be seen by substituting these values in Eq. (1).

Effects of boundary conditions on the shear strength of 0°–0° rock joints are compared with rock joints having regular i.e. 15°–15°, 30°–30° and irregular i.e. 30°–15° triangular asperities. The percentage (%) increase in shear strength for different asperity at different P_i for both CNL and CNS conditions are plotted in Fig. 11. It is observed that the shear strength increases with increase in asperity angle because of increased frictional resistance offered by the asperity. But the % increase in peak shear stress decreases with increase in P_i for both CNL and CNS conditions, it is due to degradation in asperity under that normal stress. The percentage of increase in shear strength from 0° to 0° joint to 15°–15° and 30°–

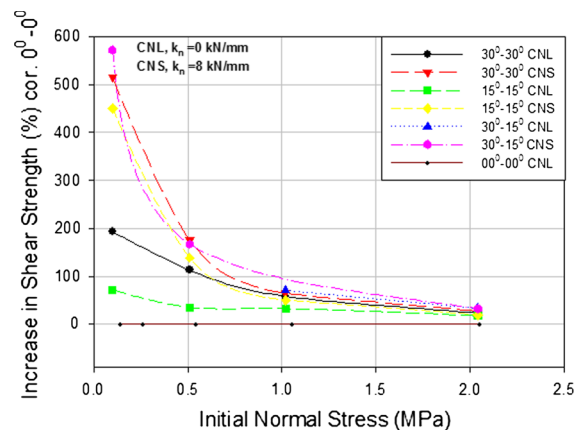


Fig. 11 Increase in shear strength under CNS conditions for different asperity with increasing P_i

30° are 71.42 and 192.85 respectively for CNL conditions at $P_i = 0.10$ MPa. It reduces to 17.56 and 23.41 % when P_i increased to 2.04 MPa for the above condition. Similarly, for CNS condition the percentage increase in shear strength from 0° to 0° to 15° to 15°, 30° to 30° and 30° to 15° are 450.00, 514.28, and 571.43 respectively for $P_i = 0.10$ MPa. The above% increase reduces to 19.51, 23.41 and 32.19 respectively when P_i is increased to 2.04 MPa.

The CNS condition shows a strain softening behaviour where as CNL condition strain hardening behaviour. The strain hardening and softening behaviour for CNL and CNS boundary condition is seen when the sheared sample crosses the peak of the asperity i.e. for 30°–30° asperity joint at shear displacement more than 8.66 mm as shown in Fig. 7. The strain softening behaviour for the CNS condition is due to decrease in normal stress during shearing when the sheared sample crosses the peak of the asperity. The strain hardening behaviour for the CNL conditions can be attributed to deposition of the sheared material within depressed portion of the joints, which has resulted into increase in shear stress.

The normal stress on the shear plane remains constant during testing for CNL conditions. However, for CNS conditions normal stress increases as asperity slides one above the other. The results show that the normal stress increases with shear displacement and reaches to the maximum value at shear displacement near to peak of the asperity i.e. 8.66 mm and after that the normal stress decreases to reach to the minimum value which is equal to initial normal stress at shear displacement equal to length of one asperity i.e. 17.32 mm as shown in Fig. 12 for 30°–30° asperity. In the CNS boundary condition variation of normal stress follows the shape of the asperity. The percentage increase in normal stress is very high about 900 % at low P_i i.e. $P_i = 0.10$ MPa and at $P_i > 0.51$ MPa the increase in normal stress is negligible for the entire asperity angle as depicted in Fig. 13.

4 New Shear Strength Model

4.1 Back Ground for Development of New Model

Classical theory proposed by Newland and Allely (1957) and Withers (1964) indicates that roughness along with the joint surface plays a vital role in

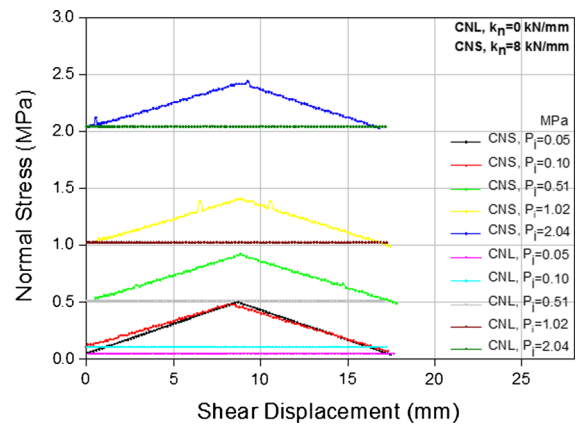


Fig. 12 Variation of normal stress of 30°–30° joints under CNL and CNS condition

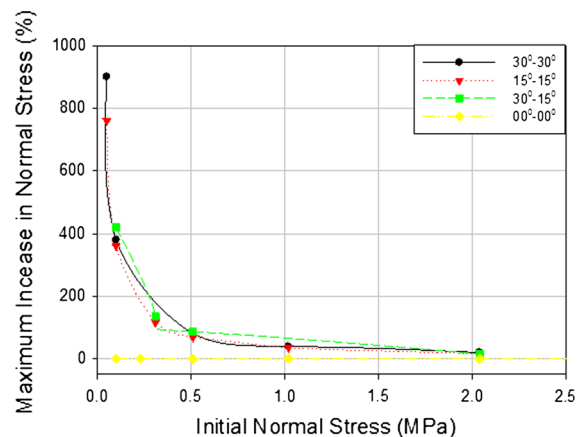


Fig. 13 Effect of asperity in % increase normal stress under CNS conditions

contributing the shear strength of rock joints. Based on a series of direct shear tests performed under CNL conditions on artificial joint specimens with regular teeth inclinations at different P_i , Patton (1966) proposed the following bilinear strength model.

$$\tau = P_i \tan(\phi_b + i) \tag{2}$$

where P_i , Φ_b and i are the initial normal stress, basic friction angle and asperity angle of the joint surface respectively.

The above Eq. (2) is valid when dilation is not restricted, joint is subjected to low normal stress and degradation of the joint surface does not take place during shearing.

If dilation is inhibited and normal stress is high the degradation of asperities occurs and shearing will take place across the asperity. This means asperity angle

changes with normal stress for CNL condition. Therefore, some researchers in the past tried to relate reduction in asperity angle with normal stress and other joint parameters. Instead of dilation angle in Eq. (2), Barton (1973) and Maksimovic (1996) has proposed the term $JRC \log (JCS/\sigma_n)$ and $\Delta\Phi(1 + \sigma_n/P_n)$ respectively. But these modifications do not account for change in normal stress during the shearing process for CNS conditions.

4.2 Development of New Shear Strength Model

The shear stress and shear displacement behaviour of modelled rock joint can be divided into three zones, different zones of one typical 30°–30° asperities is presented in Fig. 14. In zone I predominantly sliding of the sample take place without shearing of the asperity. The limit of the zone-I depends upon the shear strength of the material and shear stress increases at higher rate with small shear displacement in this zone. The angle of friction of the model material is 45°, which limits the zone-I at shear stress = P_i . In zone-II, shearing of the asperity is more predominant than the sliding. The limit of the zone-II is up to maximum shear stress, in this zone rate of increase in shear stress decreases with shear displacement. Zone-III is the last zone where all the asperity is sheared off. Due to deposition of the crushed material on the joints, shear stress decreases or increases slightly with shear displacement depending upon CNL or CNS conditions.

The shear test results on planar rock joint i.e. 0°–0° asperity modelled rock joint reflects that the strength

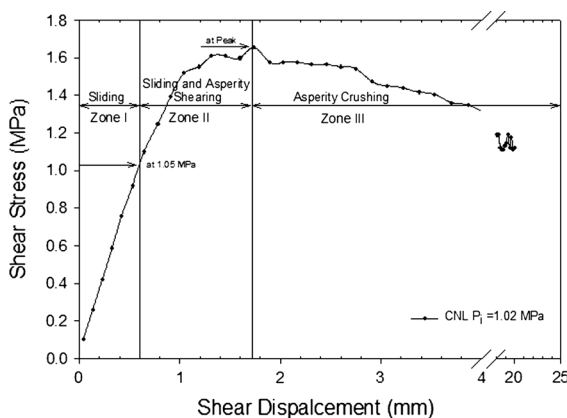


Fig. 14 Different zones of shearing

envelope for the CNL boundary condition is linear for all range of initial normal stress. Where as for non planar rock joint i.e. 15°–15°, 30°–15° and 30°–30° asperities the strength envelope is curvilinear for both CNL and CNS boundary condition and the curvature of the strength envelope increases with increase in asperity angle as presented in Fig. 15. The curvature of the strength envelopes also change with change in the initial normal stress for non planar joint. The curvature of the strength envelope is same up to low normal stress i.e. $P_i \leq 0.09 \sigma_c$ and after that the curvature of the strength envelope is increased and approaches more towards the linearity for both CNL and CNS conditions. At $P_i > 0.09 \sigma_c$ and $P_i < 0.18 \sigma_c$, the shear strength increases with increase in the asperity angle. But increase in the P_i reduces the effect of the asperity angle on increasing the shear strength. The reasons for above are degradation of the asperity angle at high normal stress and joints behave almost like a planar joint. At high initial normal stress i.e. $P_i > 0.18 (\sigma_c)$, there is no effect of the asperity angle and boundary condition on the shear strength.

On the basis of experimental observations and results, a shear strength model is developed. Bilinear shear strength model proposed by Patton (1966) is used as a basic equation, for the development of the present model. The two major limitations of Eq. (2) is presented below:

1. unable to use correct value of P_i for CNS conditions,
2. the effect of asperity degradation is not considered due to increase in normal stress.

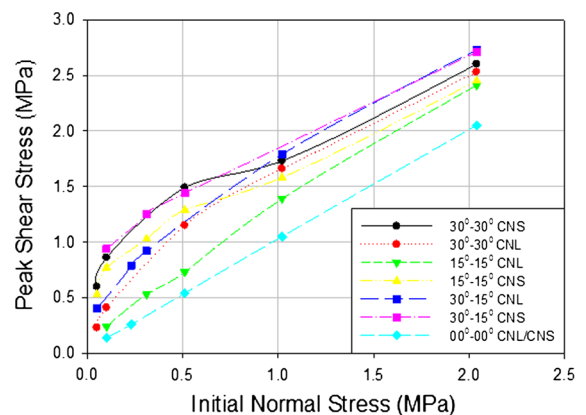


Fig. 15 Comparison of strength envelopes of different asperity (CNL and CNS)

Hence, Eq. (2) is modified to overcome the above limitations. It is developed by assuming that at peak shear stress under CNS condition, normal stress momentarily remains constant. The equation is as given below:

$$\tau_p = P_n \tan(\varphi_b + i') \tag{3}$$

where τ_p = peak shear stress in MPa, P_n = normal stress corresponding to peak shear stress in MPa for CNL/CNS condition, φ_b = basic friction angle ($^\circ$), i' = effective asperity angle ($^\circ$).

4.2.1 Prediction Model for Normal Stress (P_n)

The increase in normal stress under CNS conditions is governed by the stiffness of the surrounding rock joint and dilation resisted during shearing. The linear variation of the normal stress is observed during shearing in the present study and similar observation is made by Jiang et al. (2004), Shrivastava and Rao (2010, 2011), Shrivastava et al. (2011) and Shrivastava (2012). The variation of normal stress corresponding to peak shear stress with P_i for different stiffness and asperity angles are presented in Fig. 16. The data fitting of the graph indicates that there is a linear relationship between the normal stress corresponding to peak shear stress and P_i as shown by Eq. (4).

$$P_n = aP_i + b \tag{4}$$

where P_n is normal stress corresponding to peak shear stress, P_i is initial normal stress in MPa, a and b are constant which depend upon the asperity angle (i) and normal stiffness (k_n).

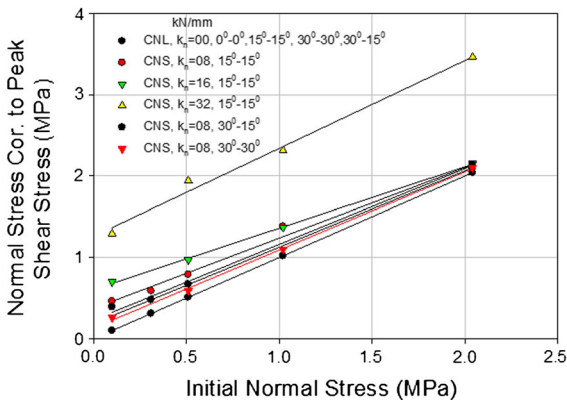


Fig. 16 Variation of normal stress for different asperity angle

The coefficient a and b along with coefficient of determination (R^2) is given in Table 2, it can be seen that constant ‘ a ’ is almost insensitive to k_n and asperity angle and hence $a = 1$ is used for all the conditions. But, the coefficient b is sensitive to both k_n and i , it decreases with increase in asperity angle and linear relationship exist between coefficient, b and k_n . The increase in asperity angle causes increase in dilation and reduction in dilation resisted which in turn reduces the increase in normal stress. Hence the generalized coefficients are:

$$a = 1 \tag{5}$$

$$b = 0.6(k_n/i) \tag{6}$$

where k_n is normal stiffness of the joint in kN/mm, i is the asperity angle ($^\circ$).

The experimentally determined normal stress (P_n) is compared with the proposed model of different asperity joint at different normal stiffness conditions and the variations of results are presented in Fig. 17. It can be seen that variation of predicted results are within 95 % of prediction band.

4.2.2 Prediction Model for Effective Asperity Angle (i')

The fine observation of the sheared samples shows that at low normal stress, sliding of the sample takes place with shear displacement and increase in normal stress causes degradation of the asperity as discussed in Sects. 3.3.1 and 4.2. The rate of asperity degradation depends upon the ratio of P_n/σ_c . Increase in this ratio causes flattening of the asperity and the reduction in the effective asperity angle. The decay rate of asperity angle is exponential as shown in Fig. 18, the figure shows that most of the experimental data falls within the 95 % confidence band. This can be represented by the following equation:

$$\frac{i'}{i} = 1.25e^{-9.86\frac{P_n}{\sigma_c}} \tag{7}$$

where i' = effective asperity angle, i = initial asperity angle, P_n = normal stress corresponding to peak shear stress, σ_c = uniaxial compressive strength in MPa.

Now, P_n and i' are calculated from the Eqs. (4) and (7) respectively. These values are substituted in the Eq. (3) to predict the shear strength under CNL and

Table 2 Coefficients for calculation of normal stress

Asperity angle (i) ($^{\circ}$)	Normal stiffness k_n (kN/mm)	a	b	R^2
00–00	0 (CNL)	1	0	1
15–15	0 (CNL)	1	0	1
	8 (CNS)	0.865	0.373	0.988
	16 (CNS)	0.753	0.606	0.999
	32 (CNS)	1.081	1.258	0.989
30–30	0 (CNL)	1	0	1
	8 (CNS)	0.958	0.133	0.998
30–15	0 (CNL)	1	0	1
	8 (CNS)	0.929	0.232	0.996

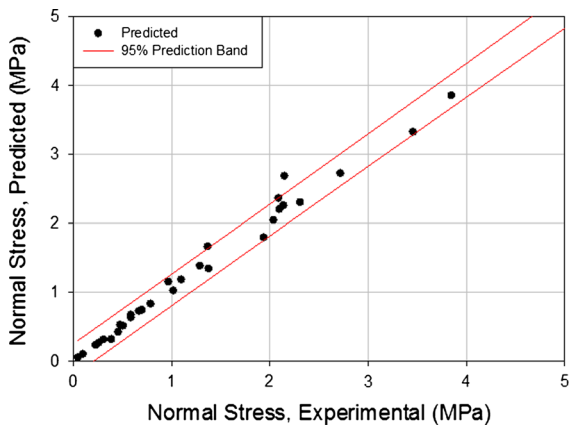


Fig. 17 Variation of predicted normal stress (P_n) from experimental results

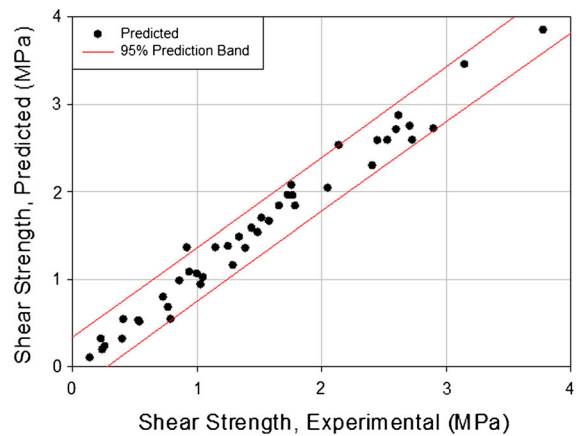


Fig. 19 Variation of predicted shear strength from experimental results

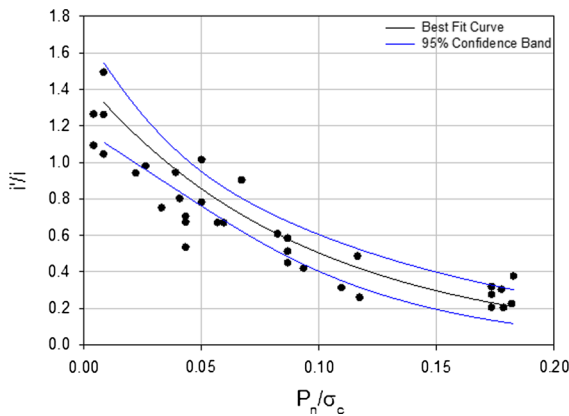


Fig. 18 Asperity decay with increase in normal stress for CNL and CNS conditions

CNS conditions. To predict the basic parameters like Φ_b , σ_c and k_n are required for any rock joints, which can be easily determined by simple testing facility or

data available in the literature for different types of rock. The asperity angle (i) is either measured or can be calculated from JRC values by the method suggested by Maksimovic (1996), which can be approximated to $i = 2 \times JRC$. The predicted peak shear stress of proposed model is compared with the experimental results and the variations of the results are plotted in Fig. 19. It can be observed that most of the predictions are within the prediction band of 95%. The predicted peak stress and normal stress for different boundary conditions is compared with the experimental results and model proposed by Patton (1966) and Barton (1973), which is presented in Table 3. The shear strength predicted by proposed model is closer to experimental value for both CNL and CNS conditions. But shear strength predicted by Patton (1966) and Barton (1973) gives comparable results only in case of CNL conditions (i.e. $k_n = 0$) but

Table 3 Experimental and predicted results of peak shear stress and normal stress

Asperity angle (i) (°)	k _n (kN/ mm)	P _i (MPa)	τ _p exp. (MPa)	P _n exp. (MPa)	P _n pred. (MPa)	τ _p pred. (MPa)	τ _p Barton (1973) (MPa)	τ _p Patton (1966) (MPa)
15–15	0	0.10	0.24	0.10	0.10	0.19	0.18	0.17
15–15	0	0.31	0.53	0.31	0.31	0.53	0.47	0.54
15–15	0	0.51	0.73	0.51	0.51	0.79	0.73	0.88
15–15	0	1.02	1.39	1.02	1.02	1.35	1.35	1.77
15–15	0	2.04	2.41	2.04	2.04	2.30	2.49	3.53
15–15	8	0.1	0.77	0.46	0.42	0.68	0.18	0.17
15–15	8	0.31	1.03	0.59	0.63	0.94	0.47	0.54
15–15	8	0.51	1.29	0.79	0.83	1.16	0.73	0.88
15–15	8	1.02	1.58	1.38	1.34	1.66	1.35	1.77
15–15	8	2.04	2.45	2.09	2.36	2.58	2.49	3.53
15–15	16	0.1	1.00	0.70	0.74	1.06	0.18	0.17
15–15	16	0.51	1.34	0.97	1.15	1.48	0.73	0.88
15–15	16	1.02	1.77	1.37	1.66	1.95	1.35	1.77
15–15	16	2.04	2.62	2.15	2.68	2.87	2.49	3.53
15–15	32	0.1	1.52	1.29	1.38	1.70	0.18	0.17
15–15	32	0.51	1.76	1.94	1.79	2.07	0.73	0.88
15–15	32	1.02	2.14	2.31	2.30	2.53	1.35	1.77
15–15	32	2.04	3.15	3.46	3.32	3.46	2.49	3.53
30–30	0	0.05	0.23	0.05	0.05	0.31	0.30	0.19
30–30	0	0.1	0.41	0.1	0.1	0.54	0.40	0.37
30–30	0	0.51	1.15	0.51	0.51	1.36	1.12	1.90
30–30	0	1.02	1.66	1.02	1.02	1.84	1.83	3.81
30–30	0	2.04	2.53	2.04	2.04	2.59	3.07	7.61
30–30	8	0.1	0.86	0.26	0.26	0.98	0.40	0.37
30–30	8	0.51	1.49	0.59	0.67	1.53	1.12	1.90
30–30	8	1.02	1.73	1.1	1.18	1.96	1.83	3.81
30–30	8	2.04	2.60	2.1	2.2	2.71	3.07	7.61
30–15	0	0.05	0.40	0.05	0.05	0.31	0.30	0.19
30–15	0	0.23	0.79	0.23	0.23	0.92	0.65	0.86
30–15	0	0.31	0.92	0.31	0.31	1.07	0.79	1.16
30–15	0	1.02	1.79	1.02	1.02	1.84	1.83	3.81
30–15	0	2.04	2.73	2.04	2.04	2.59	3.07	7.61
30–15	8	0.1	0.94	0.39	0.26	0.98	0.40	0.37
30–15	8	0.31	1.25	0.48	0.47	1.31	0.79	1.16
30–15	8	0.51	1.73	0.67	0.67	1.53	1.12	1.90
30–15	8	2.04	2.71	2.14	2.2	2.71	3.07	7.61
0–0	0	0.1	0.14	0.1	0.1	0.10	0.10	0.10
0–0	0	0.23	0.26	0.23	0.23	0.23	0.23	0.23
0–0	0	0.51	0.54	0.51	0.51	0.51	0.51	0.51
0–0	0	1.02	1.05	1.02	1.02	1.02	1.02	1.02
0–0	0	2.04	2.05	2.04	2.04	2.04	2.04	2.04
0–0	0	2.72	2.9	2.72	2.72	2.72	2.72	2.72
0–0	0	3.85	3.78	3.85	3.85	3.85	3.85	3.85

Table 4 Validation of proposed model for different rock samples (CNS)

Description of sample	σ_c (MPa)	k_n (kN/mm)	i (°)	P_i (MPa)	τ_p exp. (MPa)	τ_p prop. (MPa)	References
Gypsum plaster	20.0	15.0	4.6	0.35	0.72	0.83	Jeong et al. (2010)
	20.0	15.0	4.6	0.70	0.95	1.11	
	20.0	15.0	4.6	1.05	1.35	1.39	
Resin concrete	107.7	108.0	4.5	2.00	4.22	3.66	Jiang et al. (2004)
	107.7	108.0	4.5	5.00	5.59	6.10	
Johnstone	3.5	26.9	10.0	0.40	0.86	0.68	Seidel and Haberfield (2002)
	3.5	35.9	5.0	0.40	0.48	0.52	
	3.5	35.9	10.0	0.40	0.64	0.52	
	3.5	35.9	15.0	0.40	0.72	0.53	
Plaster of Paris	12.0	8.5	18.5	0.05	1.30	0.88	Indraratna et al. (1998)
	12.0	8.5	18.5	0.16	1.36	1.05	
	12.0	8.5	18.5	0.30	1.86	1.34	
	12.0	8.5	18.5	0.56	2.25	1.85	
	12.0	8.5	18.5	1.10	2.44	2.31	
	12.0	8.5	18.5	1.64	3.12	3.01	
	12.0	8.5	18.5	2.43	0.49	0.66	
	12.0	8.5	9.5	0.16	0.66	0.82	
	12.0	8.5	9.5	0.30	1.01	1.10	
	12.0	8.5	9.5	0.56	1.54	1.64	
	12.0	8.5	9.5	1.10	1.80	2.14	
	12.0	8.5	9.5	1.63	2.72	2.89	
	12.0	8.5	9.5	2.43	1.07	1.02	
	12.0	8.5	26.5	0.05	1.14	1.18	
	12.0	8.5	26.5	0.16	1.61	1.35	
	12.0	8.5	26.5	0.30	1.68	1.61	
12.0	8.5	26.5	0.56	2.05	2.07		
12.0	8.5	26.5	1.10	2.82	2.48		
12.0	8.5	26.5	1.63	3.35	3.12		
12.0	8.5	26.5	2.43	0.86	0.68		

for CNS conditions (i.e. $k_n > 0$) the results are under predicted.

The Proposed model is validated with some of the experimental results available on natural and artificial rock joints in the literature. As the proposed model require basic parameters like Φ_b , σ_c , and i , where ever these parameters are not reported in the experimental results by different researcher than, for JRC value equivalent asperity angle (i) is calculated by the method suggested by Maksimovic (1996) and for Φ_b , σ_c the value available in the literature for different types of

rock is used. Shear strength reported in literature based on experimentation for different types of rock or model material is also predicted by proposed Eq. (3), comparison of results are presented in Tables 4 and 5 for CNS and CNL conditions respectively, the predicted results are in very close agreements with experimental value for both the boundary conditions. The regression analysis has been done for the results presented in Table 4 and presented in Fig. 20, it can be observed that the proposed model has predicted the results within the prediction band of 95 %.

Table 5 Validation of proposed model for different rock samples (CNL)

Description of sample	Φ_b (°)	σ_c (MPa)	P_1 (MPa)	JRC	τ_p prop. (MPa)	τ_p exp. (MPa)	References
Limestone 1 (rough fracture)	35.7	26	0.50	17.1	1.46	1.08	Asadollahi and Tonon (2010)
	35.7	26	1.50	14.3	2.22	2.53	
Sandstone (rough fracture)	31.4	41	0.50	15.0	1.06	0.82	
	31.4	41	1.00	8.9	1.15	1.00	
	31.4	41	1.50	5.9	1.34	1.23	
Granite (rough fracture)	24.3	138	1.00	16.2	1.88	1.56	
	24.3	138	1.50	17.7	3.08	2.33	
	24.3	138	2.00	19.4	4.57	3.19	
Limestone 2 (rough fracture)	39.2	155	0.50	9.1	0.91	0.92	
	39.2	155	1.00	9.3	1.81	1.67	
	39.2	155	2.00	10.1	3.67	3.17	
Limestone 1 sawed	35.7	26	1.00	1.0	0.76	0.75	
	35.7	26	5.00	1.0	3.64	3.52	
	35.7	26	0.50	1.0	0.39	0.33	
	35.7	26	1.00	1.0	0.76	0.73	
	35.7	26	2.00	1.0	1.50	1.54	
	35.7	26	4.00	1.0	2.93	3.10	
	35.7	26	5.00	1.0	3.64	3.50	
Sandstone sawed	35.7	26	3.00	1.0	2.22	2.10	
	31.4	41	0.50	1.0	0.33	0.39	
	31.4	41	1.00	1.0	0.66	0.76	
	31.4	41	1.50	1.0	0.98	0.88	
	31.4	41	0.60	1.0	0.40	0.42	
	31.4	41	1.20	1.0	0.79	0.79	
Granite sawed	31.4	41	2.00	1.0	1.30	1.40	
	24.9	138	4.00	1.0	2.02	1.79	
Limestone 2 sawed	24.9	138	2.50	1.0	1.27	1.35	
	39.2	155	0.60	1.0	0.53	0.58	
Gneiss	39.2	155	0.80	1.0	0.71	0.71	
	39.2	155	0.70	1.0	0.62	0.59	
	39.2	155	0.90	1.0	0.80	0.72	
	39.2	155	1.10	1.0	0.97	0.83	
	39.2	155	1.30	1.0	1.15	0.98	
	36.0	184	1.90	12.9	4.10	3.40	
Granite	36.0	184	3.52	7.4	4.40	4.00	Grasselli and Egger (2003)
	36.0	184	3.57	6.7	4.23	3.90	
	36.0	184	3.52	8.6	4.81	4.30	
	36.0	184	4.08	1.8	3.38	3.30	
	36.0	184	2.60	9.4	3.92	3.50	
	36.0	87	0.87	13.0	1.90	1.71	
Gneiss	34.0	173	1.12	14.2	2.68	2.40	
	34.0	173	1.12	15.9	3.31	2.90	
Granite	34.0	173	2.65	3.3	2.31	2.40	

Table 5 continued

Description of sample	Φ_b (°)	σ_c (MPa)	P_i (MPa)	JRC	τ_p prop. (MPa)	τ_p exp. (MPa)	References
Concrete replica	30.0	30	0.035	0.0	0.02	0.02	Desai and Fishman (1991)
	30.0	30	0.138	0.0	0.08	0.08	
	30.0	30	0.345	0.0	0.20	0.20	
	30.0	30	0.035	0.0	0.02	0.02	
	30.0	30	0.069	0.0	0.04	0.04	
	30.0	30	0.138	0.0	0.08	0.09	

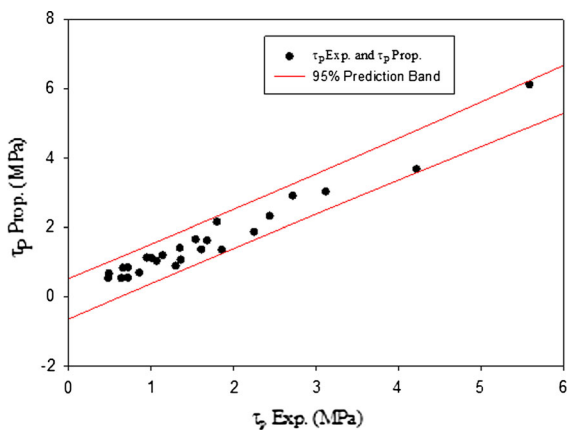


Fig. 20 Variation of predicted shear strength from results available in the literature for CNS conditions

5 Conclusions

Direct shear tests have been performed on physically modeled rock joints with asperity angle 30°–30°, 15°–15°, 30°–15° and 0°–0° under CNL and CNS conditions at different P_i to study the effect of normal stiffness and roughness of the rock joints on shear behavior. It is observed that normal load on the shearing plane is constant under CNL conditions and it increases under CNS conditions during shearing process. The variation of normal stress follows the profile of the asperity angle under CNS condition. The effect of asperity angle is to increase the shear strength with increase in the asperity angle and it increases more for CNS than CNL conditions, but the effect is reducing with increase in P_i . At $P_i \geq 0.18 \sigma_c$ the shear strength under CNL and CNS conditions are almost same. Asperities with irregular profile have higher shear strength than the regular profile. The strength envelope for planar joint is linear and it changes to

curvilinear for non planar joints under both CNL and CNS condition. Based on the series of tests conducted on different asperities joints under CNL and CNS conditions a new model for predicting the shear strength of rock joints is proposed. The proposed model is validated by predicting the shear strength of all types of rocks ranging from soft to hard under CNL and CNS conditions for different asperity angle or JRC value, whose experimental results are available in the literature and it is found that the proposed model successfully describes the shear strength of all the joints under both CNL and CNS conditions.

References

Asadollahi P, Tonon F (2010) Constitutive model for rock fractures: revisiting Barton’s empirical model. *Eng Geol* 113:11–32

Barton N (1973) Review of a new shear strength criterion for rock joints. *Eng Geol* 7:287–332

Byerlee JD (1975) The fracture strength and frictional strength of weber sandstone. *Int J Rock Mech Min Sci Geomech Abst* 12:1–4

Deere DU, Miller RP (1966) Engineering classification and index properties of rock. Technical report no. AFNL-TR-65-116. Air Force Weapons Laboratory, Albuquerque

Desai CS, Fishman KL (1991) Plasticity-based constitutive model with associated testing for joints. *Int J Rock Mech Min Sci Geomech Abst* 28:15–26

Ghazvinian AH, Taghichian A, Hashemi M, Mar’ashi SA (2010) The shear behaviour of bedding planes of weakness between two different rock types with high strength difference. *Rock Mech Rock Eng* 43:69–87

Goldestin M, Gooser B, Pyrogovsky N, Tulinov R, Turovskaya A (1966) Investigation of mechanical properties of cracked rock, vol 1. In: Proceedings of the 1st congress international society in rock mechanics, Lisbon, pp 521–524

Grasselli G, Egger P (2003) Constitutive law for the shear strength of rock joints based on three-dimensional surface parameters. *Int J Rock Mech Min Sci Geomech* 40:25–40

- Indraratna B, Haque A, Aziz N (1998) Laboratory modelling of shear behaviour of soft joints under constant normal stiffness condition. *J Geotech Geol Eng* 16:17–44
- ISRM (1977) Suggested method for determining water content, porosity, density, absorption and related properties and swelling and slake-durability index properties. Pergamon Press
- ISRM (1979) Suggested method for determining the uniaxial compressive strength and deformability of rock materials. Pergamon Press
- Jeong S, Ahn S, Seol H (2010) Shear load transfer characteristics of drilled shafts socketed in rocks. *Rock Mech Rock Eng* 43:41–54
- Jiang Y, Xiao J, Tanabashi Y, Mizokami T (2004) Development of an automated servo-controlled direct shear apparatus applying a constant normal stiffness condition. *Int J Rock Mech Min Sci* 41:275–286
- Kim DY, Chun BS, Yang JS (2006) Development of a direct shear apparatus with rock joints and its verification tests. *Geotech Test J* 29(5):1–9
- Ladanyi B, Archambault G (1970) Simulation of shear behaviour of a jointed rock mass. In: Proceedings of 11th symposium on rock mechanics: theory and practice. American Institute of Mining, Metallurgical and Petroleum Engineers, New York, pp 105–125
- Maksimovic M (1996) The shear strength components of a rough rock joint. *Int J Rock Mech Min Sci Geomech Abstr* 33:769–783
- Newland PL, Allely BH (1957) Volume changes in drained triaxial tests on granular materials. *Geotechnique* 7:17–34
- Obert L, Brady BT, Schmechel FW (1976) The effect of normal stiffness on the shear resistance of rock. *Rock Mech* 8(2):57–72
- Ooi LH, Carter PJ (1987) A constant normal stiffness direct shear device for static and cyclic loading. *Geotech Test J* 10(1):3–12
- Patton FD (1966) Multiple modes of shear failure in rock and related materials. Dissertation, University of Illinois, Urbana
- Rao KS, Shrivastava AK, Singh J (2009) Development of an automated large scale direct shear testing machine for rock. In: Indian geotechnical conference, pp 238–244
- Saiang D, Malmgren L, Nordlund E (2005) Laboratory tests on shortcrete rock joints in direct shear, tension and compression. *Rock Mech Rock Eng* 38:275–297
- Seidel JP, Haberfield CM (2002) A theoretical model for rock joints subjected to constant normal stiffness direct shear. *Int J Rock Mech Min Sci Geomech Abstr* 39:539–553
- Shrivastava AK (2012) Physical and numerical modelling of shear behaviour of jointed rocks under CNL and CNS boundary conditions. Dissertation, IIT Delhi
- Shrivastava AK, Rao KS (2010) Effect of boundary conditions on shear behaviour of rock joint. In: ISRM international symposium and 6th Asian rock mechanics symposium—advances in rock engineering, New Delhi, India
- Shrivastava AK, Rao KS (2011) Shear behaviour of non planar rock joint. In: 14th Asian regional conference on soil mechanics and geotechnical engineering, Hong Kong
- Shrivastava AK, Rao KS (2013) Development of a large-scale direct shear testing machine for unfilled and infilled rock joints under constant normal stiffness conditions. *Geotech Test J* 36(5):670–679
- Shrivastava AK, Rao KS, Rathod GW (2011) Shear behaviour of rock under different normal stiffness. In: 12th international congress on rock mechanics (ISRM), Beijing, pp 831–835
- Withers JH (1964) Sliding resistance along discontinuities in rock mass. Dissertation, University of Illinois
- Xie H, Pariseau WG (1992) Fractal estimate of joint roughness coefficients. In: Proceedings of the international conference on fractal and jointed rock masses, Lake Tahoe, CA, pp 125–131
- Yang ZY, Chiang DY (2000) An experimental study on the progressive shear behaviour of rock joints with tooth-shaped asperities. *Int J Rock Mech Min Sci* 37:1247–1259